

## Mössbauer Spectroscopic Studies of Trialkyl- and Triaryltin Complexes of Transition Metal Cyanides

Motomi KATADA,\* Yoshio UCHIDA, Kumiko IWAI, Hirotoishi SANO,  
Hiroshi SAKAI,<sup>†</sup> and Yutaka MAEDA<sup>†</sup>

Department of Chemistry, Faculty of Science, Tokyo Metropolitan University,  
Fukasawa, Setagaya-ku, Tokyo 158

<sup>†</sup>Research Reactor Institute, Kyoto University, Kumatori-cho, Sennan-gun, Osaka 590-04  
(Received August 30, 1986)

The structural diagnosis and lattice dynamics of three complexes,  $\{[R_3Sn](\mu\text{-NC})[Au(\mu\text{-CN})]\}_x$  ( $R=\text{Me}$ ,  $\text{Bu}(n\text{-Bu})$ , or  $\text{Ph}$ ),  $\{[R_3Sn]_2[(\mu\text{-NC})_4Pt]\}_x$  ( $R=\text{Me}$ ,  $\text{Bu}$ , or  $\text{Ph}$ ), and  $\{[R_3Sn]_3[(\mu\text{-NC})_6Fe]\}_x$  ( $R=\text{Bu}$  or  $\text{Ph}$ ) have been undertaken by means of  $^{57}\text{Fe}$ -,  $^{119}\text{Sn}$ -, and  $^{197}\text{Au}$ -Mössbauer spectroscopic techniques. The Mössbauer parameters for the complexes indicate that all the tin atoms are coordinated with three alkyl or aryl groups and two cyano groups having a trigonal-bipyramidal structure. The asymmetry of the quadrupole split-peak intensity observed in the  $^{119}\text{Sn}$ -Mössbauer spectra for the complexes was attributed to the anisotropic mean square vibrational amplitude with respect to a molecular symmetry axis. The temperature dependence of the recoil-free fraction of the  $^{119}\text{Sn}$ -Mössbauer atom shows that the mean-square vibrational amplitude of tin atoms in the complexes falls in the range of values found for a number of one-dimensional organotin polymers. In  $^{57}\text{Fe}$ -Mössbauer spectroscopy, the quadrupole splitting for  $\{[Bu_3Sn]_3[(\mu\text{-NC})_6Fe]\}_x$  rapidly decreases with an increase in the temperature, reflecting small separations among the three  $d_e$  levels in energy. The very large  $^{197}\text{Au}$ -quadrupole splitting for  $\{[R_3Sn](\mu\text{-NC})[Au(\mu\text{-CN})]\}_x$  was explained by assuming strong  $\sigma$ -donating and  $\pi$ -accepting properties of the CN ligand.

Recently, Uson et al. synthesized various kinds of trialkyl- and triaryltin complexes of transition metal cyanides by treating the trialkyl- or triaryltin perchlorates with several cyano compounds of transition metals.<sup>1)</sup> If the reaction with anionic dicyano compounds, such as  $K[Au(CN)_2]$  and  $Bu_4N[Ag(CN)_2]$ , is carried out, the reaction products can be expected to have an infinite one-dimensional polymeric structure. On the other hand, the reaction with the square-planar coordinated palladium or platinum cyanides can be expected to give polymer complexes which are assumed to have an infinite two-dimensional structure. In the case of the reaction with  $K_3[Fe(CN)_6]$ , three-dimensional polymer products will be obtained.

On the basis of the IR spectra of those complexes, Uson et al. proposed that, in every case, the tin atoms are five-coordinated with three alkyl or aryl groups in the equatorial position and two cyano groups in the axial position of a trigonal-bipyramidal and that the tin and the transition metal are bridged by a cyano group.

Mössbauer spectroscopy can provide valuable information about the nature of chemical bonding and the structures of compounds containing "Mössbauer-active atoms," such as tin, iron, and gold, because Mössbauer parameters are very sensitive to the number and nature of ligands coordinated to the Mössbauer atoms.<sup>2–4)</sup> Especially,  $^{197}\text{Au}$ -Mössbauer spectroscopy is one of the most powerful techniques in the structural diagnosis of the gold compounds. In the present study,  $^{57}\text{Fe}$ -,  $^{119}\text{Sn}$ -, and  $^{197}\text{Au}$ -Mössbauer spectroscopic studies have been undertaken in order to examine the coordination for the iron, tin, and gold atoms and to elucidate the lattice dynamical proper-

ties of tin and iron sites in the trialkyl- and triaryltin complexes of transition metal cyanides, such as  $\{[R_3Sn](\mu\text{-NC})[Au(\mu\text{-CN})]\}_x$  and  $\{[R_3Sn]_2[(\mu\text{-NC})_4Pt]\}_x$  ( $R=\text{Me}$ ,  $\text{Bu}$ , or  $\text{Ph}$ ), and  $\{[R_3Sn]_3[(\mu\text{-NC})_6Fe]\}_x$  ( $R=\text{Bu}$  or  $\text{Ph}$ ).

### Experimental

**Materials.** All the complexes investigated were prepared by the following method, described in a reference.<sup>1)</sup> Organotin perchlorates  $R_3SnClO_4$  ( $R=\text{Me}$ ,  $\text{Bu}$ , or  $\text{Ph}$ ) were prepared in acetone by treating stoichiometric amounts of the corresponding organotin chloride,  $R_3SnCl$ , with  $AgClO_4$ . The filtrate was used for further reactions without any other treatment. The  $\{[R_3Sn](\mu\text{-NC})[Au(\mu\text{-CN})]\}_x$  complexes ( $R=\text{Me}$ ,  $\text{Bu}$ , or  $\text{Ph}$ ) were obtained by treating a solution of  $K[Au(CN)_2]$  (3 mmol) in acetone with an equimolar amount of  $R_3SnClO_4$ . The precipitates were filtered off and washed with a mixture of water and acetone. The  $\{[R_3Sn]_2[(\mu\text{-NC})_4Pt]\}_x$  ( $R=\text{Me}$ ,  $\text{Bu}$ , or  $\text{Ph}$ ) complexes were prepared by the same procedure using 3 mmol of  $K_2[Pt(CN)_4]$  and 6 mmol of  $R_3SnClO_4$ . The precipitates were washed with acetone and then hexane. The  $\{[R_3Sn]_3[(\mu\text{-NC})_6Fe]\}_x$  ( $R=\text{Bu}$  or  $\text{Ph}$ ) complexes were also prepared as has been described above by treating 3 mmol of  $K_3[Fe(CN)_6]$  with 9 mmol of  $R_3SnClO_4$ . The products were washed with acetone. The purity of the complexes was confirmed by elemental analyses for C, H, and N.

**Mössbauer Spectroscopic Measurements.** The temperature-dependent Mössbauer-effect measurements for  $^{57}\text{Fe}$  and  $^{119}\text{Sn}$  were carried out by using a constant-acceleration-type spectrometer over the temperature range of  $78\text{ K} \leq T \leq 300\text{ K}$ . Most of the  $^{119}\text{Sn}$ -Mössbauer spectroscopic measurements were carried out from 78 to about 200 K, since the recoil-free fraction of the complexes becomes too small to be measured at high temperatures. The temperature of the absorber was controlled within  $\pm 0.5\text{ K}$ .  $^{197}\text{Au}$ -Mössbauer spectroscopic measurements were carried out with a source and an

absorber, both cooled to 16 K by using a constant-acceleration-type spectrometer in connection with a pure-Ge diode detector. The details of the  $^{197}\text{Au}$ -Mössbauer spectroscopy have been described elsewhere.<sup>5)</sup>

The spectra observed were fitted with Lorentian-line shapes by using the least-squares fitting procedure. The velocity scale was calibrated by using a metallic iron-foil spectrum. The isomer shifts of the  $^{57}\text{Fe}$  and  $^{119}\text{Sn}$  spectra are reported with respect to  $\alpha\text{-Fe}$  and  $\text{BaSnO}_3$  resonances respectively at room temperature. All the isomer shifts of the  $^{197}\text{Au}$ -Mössbauer spectra are referred to metallic gold at 16 K.

### Results and Discussion

**$^{119}\text{Sn}$ -Mössbauer Spectra.** Some typical  $^{119}\text{Sn}$ -Mössbauer spectra obtained at 78 K are shown in Fig. 1 for  $\{[\text{R}_3\text{Sn}](\mu\text{-CN})[\text{Au}(\mu\text{-CN})]\}_x$  ( $\text{R}=\text{Me, Bu, or Ph}$ ), while the Mössbauer parameters, such as the isomer shift ( $IS$ ), the quadrupole splitting ( $QS$ ), and the half-width ( $\Gamma_{\text{exp}}$ ), derived from the observed spectra are summarized in Table 1. The spectra observed consist of one doublet with relatively large  $QS$  values, as may be seen in Fig. 1.

In  $^{119}\text{Sn}$ -Mössbauer spectroscopy, the major variation in the  $QS$  values observed can be attributed to the difference in the structural change. The range of  $QS$  values for organotin compounds can be classified into the following four groups:<sup>6)</sup> 1) tetrahedral  $\text{R}_n\text{SnX}_{4-n}$  ( $n=1-3$ ) [ $0.00-2.31 \text{ mm s}^{-1}$ ], 2) octahedral *cis*- $\text{R}_2\text{SnX}_4$  [ $1.63-2.34 \text{ mm s}^{-1}$ ], 3) trigonal-bipyramidal  $\text{R}_3\text{SnX}_2$  ( $\text{X}$  axial) [ $2.76-3.86 \text{ mm s}^{-1}$ ], and 4) octahedral *trans*- $\text{R}_2\text{SnX}_4$  [ $3.37-4.32 \text{ mm s}^{-1}$ ]. On the basis of this criterion, the tin atoms in the complexes under discussion can be concluded to have a five-coordinated structure, in which the tin atom is bridged by a CN group. This result is in good agreement with the hypothetical conclusion proposed by Uson et al.<sup>1)</sup> for the coordination state of tin atoms in the same compounds.

The  $QS$  values for  $\text{Ph}_3\text{Sn}$  derivatives are smaller than those of the corresponding  $\text{Me}_3\text{Sn}$  or  $\text{Bu}_3\text{Sn}$  derivatives. The decrease in the  $QS$  values for the

$\text{Ph}_3\text{Sn}$  derivatives can be explained by the greater partial  $QS$  value assigned to the phenyl group compared to that of the alkyl group. The same tendency was observed for various kinds of organotin compounds containing the phenyl group.<sup>6)</sup>

The temperature dependence of the quadrupole splitting is negligible in every case, since the  $QS$  for organotin(IV) compounds arises from mainly an inequality in the nature of the tin-ligand bonds, which is temperature-independent. However, the intensity asymmetry of the quadrupole line and its temperature dependence were observed, as is shown in

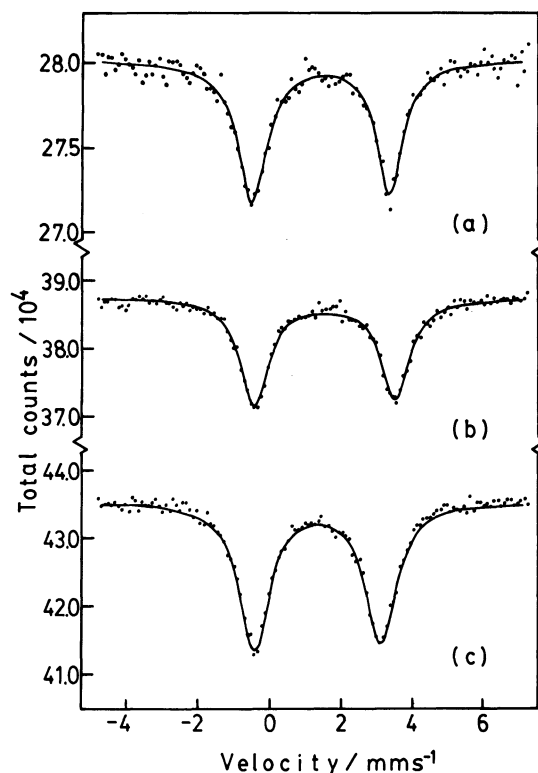


Fig. 1.  $^{119}\text{Sn}$ -Mössbauer spectra for (a)  $\{[\text{Me}_3\text{Sn}](\mu\text{-NC})[\text{Au}(\mu\text{-CN})]\}_x$ , (b)  $\{[\text{Bu}_3\text{Sn}](\mu\text{-NC})[\text{Au}(\mu\text{-CN})]\}_x$ , and (c)  $\{[\text{Ph}_3\text{Sn}](\mu\text{-NC})[\text{Au}(\mu\text{-CN})]\}_x$  at 78 K.

Table 1.  $^{119}\text{Sn}$ -Mössbauer Parameters for Trialkyl- and Triaryltin Complexes of Transition Metal Cyanides

Complex	$IS^a$	$QS^b$	$\Gamma_{\text{exp}}^b$		$\theta^2 M^c$
	$\text{mm s}^{-1}$	$\text{mm s}^{-1}$	$\text{mm s}^{-1}$	$\text{mm s}^{-1}$	$10^6 \times \text{deg}^2 \text{amu}$
$\{[\text{Me}_3\text{Sn}](\mu\text{-NC})[\text{Au}(\mu\text{-CN})]\}_x$	1.43	3.86	1.00	0.87	0.76 (78—157 K)
$\{[\text{Bu}_3\text{Sn}](\mu\text{-NC})[\text{Au}(\mu\text{-CN})]\}_x$	1.54	3.92	0.95	1.00	0.80 (78—133 K)
$\{[\text{Ph}_3\text{Sn}](\mu\text{-NC})[\text{Au}(\mu\text{-CN})]\}_x$	1.33	3.54	0.98	1.04	1.59 (78—219 K)
$\{[\text{Me}_3\text{Sn}]_2[(\mu\text{-NC})_4\text{Pt}]\}_x$	1.33	3.86	0.98	1.07	1.08 (78—179 K)
$\{[\text{Bu}_3\text{Sn}]_2[(\mu\text{-NC})_4\text{Pt}]\}_x$	1.58	4.18	1.07	1.13	1.00 (78—179 K)
$\{[\text{Ph}_3\text{Sn}]_2[(\mu\text{-NC})_4\text{Pt}]\}_x$	1.36	3.90	1.09	1.09	1.25 (78—179 K)
$\{[\text{Bu}_3\text{Sn}]_3[(\mu\text{-NC})_6\text{Fe}]\}_x$	1.49	3.86	0.98	1.16	1.00 (78—145 K)
$\{[\text{Ph}_3\text{Sn}]_3[(\mu\text{-NC})_6\text{Fe}]\}_x$	1.29	3.35	0.99	1.17	1.33 (78—195 K)

a) Relative to  $\text{BaSnO}_3$ ;  $\pm 0.02 \text{ mm s}^{-1}$ . b)  $\pm 0.02 \text{ mm s}^{-1}$ . c)  $\pm 0.05 \text{ deg}^2 \text{amu}$ .

Fig. 2 for  $\{[\text{Bu}_3\text{Sn}]_2[(\mu\text{-NC})_4\text{Pt}]]_x$ . This asymmetry is commonly found in one- and two-dimensional polymeric compounds.<sup>7</sup> The temperature dependences of intensity asymmetry observed in other complexes are summarized graphically in Fig. 3, where  $R$  is the ratio of the areal intensity,  $A_+$ , of the

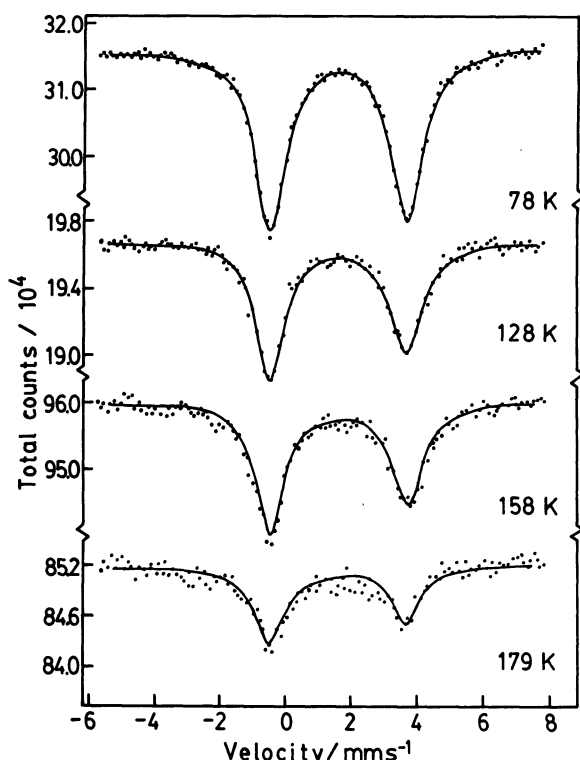


Fig. 2.  $^{119}\text{Sn}$ -Mössbauer spectra for  $\{[\text{Bu}_3\text{Sn}]_2[(\mu\text{-NC})_4\text{Pt}]]_x$  at various temperatures.

resonance peak at the higher velocity to that,  $A_-$ , of the peak at the lower velocity.

The intensity asymmetry has been theoretically expressed as a function of the difference in the mean-square vibrational amplitude parallel and perpendicular with respect to the principal axis of the electric-field gradient (EFG) tensor:<sup>9</sup>

$$R' = \frac{I(\pm 1/2 \leftrightarrow \pm 3/2)}{I(\pm 1/2 \leftrightarrow \pm 1/2)} = \frac{\int_0^\pi \exp\{-(1/\lambda^2)[\langle z^2 \rangle - \langle x^2 \rangle] \cos^2 \theta\} (1 + \cos^2 \theta) \sin \theta d\theta}{\int_0^\pi \exp\{-(1/\lambda^2)[\langle z^2 \rangle - \langle x^2 \rangle] \cos^2 \theta\} (5/3 - \cos^2 \theta) \sin \theta d\theta} \quad (1)$$

where  $\langle z^2 \rangle$  and  $\langle x^2 \rangle$  are the mean square vibrational amplitudes parallel and perpendicular respectively to the principal axis of the EFG tensor.

The more intense line can be assigned to the  $\pm 1/2 \leftrightarrow \pm 3/2$  transition by assuming that the difference in  $[\langle z^2 \rangle - \langle x^2 \rangle]$  is negative, i.e., that the vibrational motion of the tin atom in the plane of  $\text{R}_3\text{Sn}$  is larger than that along the molecular symmetry axis corresponding to the  $\text{CN-Sn-NC}$  chain. Thus, the observed intensity asymmetry suggests that the sign of the quadrupole coupling constant,  $e^2qQ$ , is negative; that is, the electric-charge distribution around a tin atom can be described as being oblate with respect to the polymer axis. This result is consistent with those for organotin compounds which have tin atoms five-coordinated in a one-dimensional chain structure in a solid.<sup>7,9-11</sup>

The observed intensity asymmetry  $R$  shown in Fig.

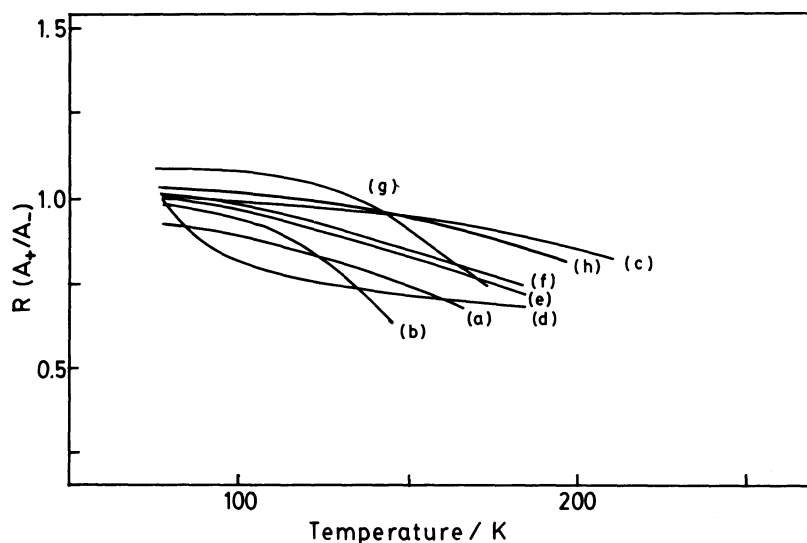


Fig. 3. Temperature dependences of peak intensity ratio for trialkyl- and triaryltin complexes of transition metal cyanides; (a)  $\{[\text{Me}_3\text{Sn}](\mu\text{-NC})[\text{Au}(\mu\text{-CN})]\}_x$ , (b)  $\{[\text{Bu}_3\text{Sn}](\mu\text{-CN})[\text{Au}(\mu\text{-CN})]\}_x$ , (c)  $\{[\text{Ph}_3\text{Sn}](\mu\text{-NC})[\text{Au}(\mu\text{-CN})]\}_x$ , (d)  $\{[\text{Me}_3\text{Sn}]_2[(\mu\text{-NC})_4\text{Pt}]]_x$ , (e)  $\{[\text{Bu}_3\text{Sn}]_2[(\mu\text{-NC})_4\text{Pt}]]_x$ , (f)  $\{[\text{Ph}_3\text{Sn}]_2[(\mu\text{-NC})_4\text{Pt}]]_x$ , (g)  $\{[\text{Bu}_3\text{Sn}]_3[(\mu\text{-NC})_6\text{Fe}]]_x$ , and (h)  $\{[\text{Ph}_3\text{Sn}]_3[(\mu\text{-NC})_6\text{Fe}]]_x$ .

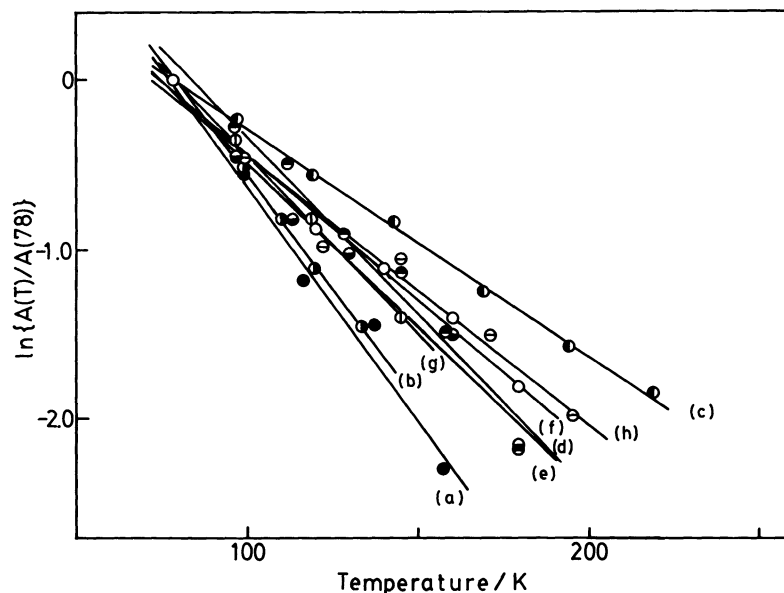


Fig. 4. Temperature dependences of the area under  $^{119}\text{Sn}$ -resonance line for (a)  $\{[\text{Me}_3\text{Sn}](\mu\text{-NC})[\text{Au}(\mu\text{-CN})]\}_x$ , (b)  $\{[\text{Bu}_3\text{Sn}](\mu\text{-NC})[\text{Au}(\mu\text{-CN})]\}_x$ , (c)  $\{[\text{Ph}_3\text{Sn}](\mu\text{-NC})[\text{Au}(\mu\text{-CN})]\}_x$ , (d)  $\{[\text{Me}_3\text{Sn}]_2[(\mu\text{-NC})_4\text{Pt}]\}_x$ , (e)  $\{[\text{Bu}_3\text{Sn}]_2[(\mu\text{-NC})_4\text{Pt}]\}_x$ , (f)  $\{[\text{Ph}_3\text{Sn}]_2[(\mu\text{-NC})_4\text{Pt}]\}_x$ , (g)  $\{[\text{Bu}_3\text{Sn}]_3[(\mu\text{-NC})_6\text{Fe}]\}_x$ , and (h)  $\{[\text{Ph}_3\text{Sn}]_3[(\mu\text{-NC})_6\text{Fe}]\}_x$ .

3 is inversely proportional to the ratio  $R'$  in Eq. 1. All the  $R$  values decrease with an increase in the temperature. This means that the mean-square vibrational amplitude in the direction perpendicular to the polymer axis depends significantly on the temperature. The temperature dependence of  $R$  for  $\text{Ph}_3\text{Sn}$  derivatives is smaller than those for  $\text{Me}_3\text{Sn}$  and  $\text{Bu}_3\text{Sn}$  derivatives. This result can be explained by assuming that the steric effect of the bulky phenyl group restricts the motion of the tin atom.

The recoil-free fraction,  $f_a$ , and its temperature dependence provide useful information about the lattice dynamical properties of a solid which are associated with the motion of Mössbauer atoms. The temperature dependences of the area under the resonance line are shown in Fig. 4 for the complexes studied in this work.

According to the Debye approximation at high temperatures, the "relative" values of the recoil-free fraction,  $f_a$ , are expressed as:

$$f_a = \exp\left(\frac{-3E_\gamma^2 T}{Mc^2 k \theta^2}\right), \quad (2)$$

where  $E_\gamma$  is the energy of the Mössbauer transition,  $\theta$  is the Debye temperature,  $M$  is the effective vibrating mass, and  $k$  is the Boltzmann constant. The temperature dependence of the recoil-free fraction,  $f_a$ , is given by Eq. 3:

$$\frac{d \ln f_a}{dT} = \frac{-3E_\gamma^2}{Mc^2 k \theta^2}. \quad (3)$$

Noting that  $k\theta/h = \nu_{\max} \propto (\alpha/M)^{1/2}$ , the following equation is obtained for the parameter of the

intermolecular force constant,  $\alpha$ :

$$\alpha \propto \theta^2 M = \frac{-3E_\gamma^2}{kc^2} \left[ \frac{d \ln f_a}{dT} \right]^{-1}, \quad (4)$$

where  $\nu_{\max}$  is the maximum lattice frequency, which is assumed to be equal to the Debye cut-off frequency, and where  $h$  is the Planck constant. The coefficient of the temperature-dependent term,  $d \ln f_a / dT$ , in Eq. 4 can be replaced for a "thin" absorber by the observed temperature dependence of the areal intensity under the resonance line (normalized to 78 K point).

It was found in our previous study that there was a distribution of the  $\theta^2 M$  values with respect to the state of molecular association in a solid.<sup>12)</sup> The values of  $\theta^2 M / 10^6 \text{ deg}^2 \text{ amu}$  are distributed around unity for a non-polymeric compound, while those of one-dimensional and two-dimensional polymeric compound are distributed around 1.3 and 1.7 respectively. The distribution of the  $\theta^2 M$  values for three-dimensional polymeric compounds may be beyond the value of the two-dimensional polymer. The distribution of the parameters can be used to determine the state of intermolecular association in a solid. Although much overlapping is observed between the non-polymeric compounds and one-dimensional polymeric compounds, and between the one-dimensional and two-dimensional polymers, the discrimination between the nonassociated and one-dimensional polymeric states and between two- and three-dimensional polymeric states can be done by detecting the asymmetric quadrupole split lines, as has been mentioned previously.

The values of  $\theta^2 M$ , as estimated from the data of the

temperature dependence of the area for the complexes, are summarized in Table 1. Although the  $\{[R_3Sn]_2[(\mu-NC)_4Pt]\}$  and  $\{[R_3Sn]_3[(\mu-NC)_6Fe]_x\}$  complexes are considered to be two- or three-dimensional polymer complexes, the values of  $\theta^2M$  in Table 1 suggest that the state of molecular association for these complexes is close to that of non-polymeric compounds or one-dimensional polymers. The values of  $\theta^2M$  for  $Me_3Sn$  and  $Bu_3Sn$  derivatives are smaller than those for  $Ph_3Sn$  derivatives in each series. This means that the motion of tin atoms in these complexes depends mainly on the ligands in the first coordination sphere of tin atoms. A large temperature dependence of the mean-square vibrational amplitude perpendicular to the polymer axis strongly affects the values of  $\theta^2M$ . The relatively large values of  $\theta^2M$  for  $Ph_3Sn$  derivatives presumably reflect the restriction on the motion of tin atoms attributable to the bulky phenyl group, which is packed rigidly in a solid. The same tendency was observed for  $R_4Sn$  compounds; e.g., the value of  $\theta^2M$  for  $Me_4Sn$  is  $0.77 \times 10^6$ , while that for  $Ph_4Sn$  is  $1.28 \times 10^6$ .<sup>12)</sup> Consequently, a comparison of the parameters of the intermolecular force constant,  $\alpha \propto \theta^2M$ , gives valuable information about the motion of tin atoms associated in a solid.

**$^{57}Fe$ -Mössbauer Spectra.** The  $^{57}Fe$ -Mössbauer spectra and their temperature dependence for  $\{[Bu_3Sn]_3[(\mu-NC)_6Fe]_x\}$  are shown in Fig. 5, while the Mössbauer parameters derived from the observed spectra are listed in Table 2. The values of  $IS$  and  $QS$  and the temperature dependence of  $QS$  indicate that the iron atom in this complex is at an Fe(III) low-spin state. The temperature dependences of  $QS$  for  $\{[Bu_3Sn]_3[(\mu-NC)_6Fe]_x\}$  and  $\{[Ph_3Sn]_3[(\mu-NC)_6Fe]_x\}$  are shown in Fig. 6.

A low-spin Fe(III) atom has a nonspheric d shell. The contribution of this configuration to the EFG

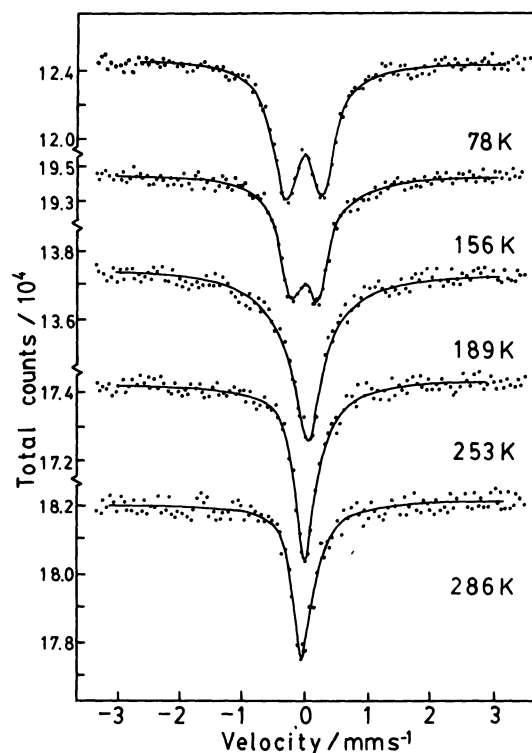


Fig. 5.  $^{57}Fe$ -Mössbauer spectra for  $\{[Bu_3Sn]_3[(\mu-NC)_6Fe]_x\}$  at various temperatures.

Table 2.  $^{57}Fe$ -Mössbauer Parameters at 78 K

Complex	$IS^a)$ mm s <sup>-1</sup>	$QS^b)$ mm s <sup>-1</sup>	$\Gamma_{exp}^b)$	
			mm s <sup>-1</sup>	mm s <sup>-1</sup>
$\{[Bu_3Sn]_3[(\mu-NC)_6Fe]_x\}$	-0.05	0.55	0.42	0.47
$\{[Ph_3Sn]_3[(\mu-NC)_6Fe]_x\}$	-0.07	1.19	0.43	0.45

a) Relative to  $\alpha$ -Fe foil;  $\pm 0.02$  mm s<sup>-1</sup>. b)  $\pm 0.02$  mm s<sup>-1</sup>.

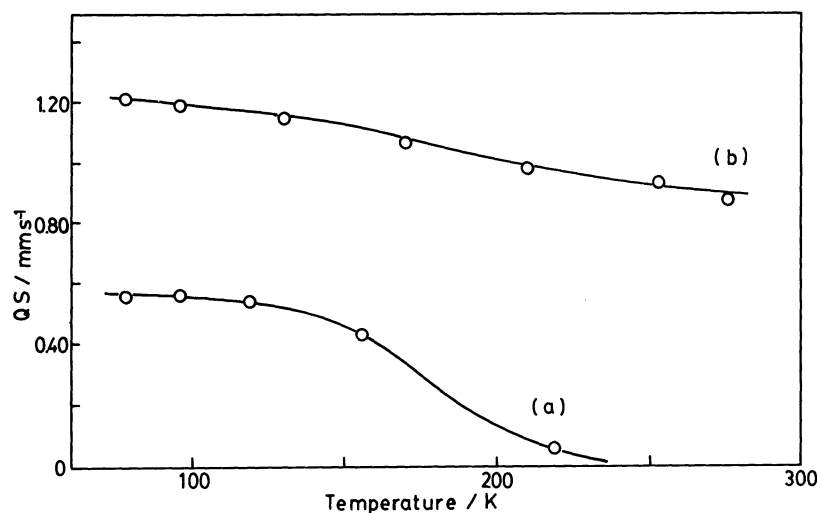


Fig. 6. Temperature dependences of the quadrupole splitting for (a)  $\{[Bu_3Sn]_3[(\mu-NC)_6Fe]_x\}$  and (b)  $\{[Ph_3Sn]_3[(\mu-NC)_6Fe]_x\}$ .

Table 3.  $^{197}\text{Au}$ -Mössbauer Parameters at 16 K

Complex	$IS^a)$	$QS^b)$	$\Gamma_{\text{exp}}^b)$	
	mm s $^{-1}$	mm s $^{-1}$	mm s $^{-1}$	mm s $^{-1}$
$\{[\text{Me}_3\text{Sn}](\mu\text{-NC})[\text{Au}(\mu\text{-CN})]\}_x$	4.51	10.45	2.00	2.00
$\{[\text{Bu}_3\text{Sn}](\mu\text{-NC})[\text{Au}(\mu\text{-CN})]\}_x$	4.37	9.99	1.93	2.17
$\{[\text{Ph}_3\text{Sn}](\mu\text{-NC})[\text{Au}(\mu\text{-CN})]\}_x$	4.45	10.08	2.01	2.01

a) Relative to Au foil;  $\pm 0.04$  mm s $^{-1}$ . b)  $\pm 0.04$  mm s $^{-1}$ .

depends on the symmetry of the external field and the temperature. A large temperature dependence of  $QS$  for the  $\text{Bu}_3\text{Sn}$  derivative indicates that the three  $d_z$  levels are close to each other in energy. The environment around iron(III) atoms is assumed to be almost cubic. On the other hand, the decrease in the  $QS$  for the  $\text{Ph}_3\text{Sn}$  derivative is slow. This can be explained by assuming that the three  $d_z$  levels are widely separated as a result of the distortion of  $\text{Fe}(\text{CN})_6$  octahedra caused by the steric hindrance of bulky phenyl groups.

The values of  $\theta^2M/10^6$  for  $^{57}\text{Fe}$  estimated by using Eq. 4 are 0.97 and 1.63 for  $\text{Bu}_3\text{Sn}$  and  $\text{Ph}_3\text{Sn}$  derivatives respectively. These values are smaller than those expected for three-dimensional polymeric compounds. This result reflects the linkage of a long  $\text{CN-Sn-NC}$  chain, which probably reduces the motional rigidity of the iron atoms in these complexes. The fact that the value for the  $\text{Ph}_3\text{Sn}$  derivative is larger than that for the  $\text{Bu}_3\text{Sn}$  derivative can be explained by the same interpretation as has been proposed for the case of  $^{119}\text{Sn}$ , that is, the motion of the iron atom is restrained by the steric effect of bulky phenyl groups. The similarity between the values of  $\theta^2M$  of  $^{57}\text{Fe}$  and those of  $^{119}\text{Sn}$  for  $\{[\text{Bu}_3\text{Sn}]_3[(\mu\text{-NC})_6\text{Fe}]\}_x$  and  $\{[\text{Ph}_3\text{Sn}]_3[(\mu\text{-NC})_6\text{Fe}]\}_x$  respectively suggests that the motion of iron atoms depends on that of tin atoms in these complexes.

**$^{197}\text{Au}$ -Mössbauer Spectroscopy.** The  $^{197}\text{Au}$ -Mössbauer spectra for the  $\{[\text{R}_3\text{Sn}](\mu\text{-NC})[\text{Au}(\mu\text{-CN})]\}_x$  complexes ( $\text{R}=\text{Me}$ ,  $\text{Bu}$ , or  $\text{Ph}$ ) consist of one doublet with quite large  $QS$  values. The Mössbauer parameters derived from the spectra are summarized in Table 3. The values of  $IS$  and  $QS$  for these complexes are very close to those of  $\text{K}[\text{Au}(\text{CN})_2]$ .<sup>13)</sup>

In linear gold(I) compounds, the  $5d_{z^2}$ ,  $6s$ , and  $6p_z$  metal orbitals (the  $z$  axis being the molecular axis) are suitable for  $\sigma$ -bonding, while the  $5d_{xz,yz}$  and  $6p_{x,y}$  orbitals are used in  $\pi$ -bonding to the ligands. The  $5d_{xy}$  and  $5d_{x^2-y^2}$  orbitals are nonbonding.  $\sigma$ -Donation into the  $5d_{z^2}$  and  $6p_z$  orbitals is expected to contribute negatively to the quadrupole coupling constant,  $e^2qQ$ . The absolute value of  $e^2qQ$  might be expected to increase the  $\sigma$ -donor strength of the ligands, assuming that the sign of  $e^2qQ$  for the two coordinated gold(I) compounds is negative. The negative  $e^2qQ$  has been confirmed experimentally for  $\text{K}[\text{Au}(\text{CN})_2]$ .<sup>14)</sup>  $\pi$ -

Bonding and  $d_\pi$ -back-bonding also affect the  $e^2qQ$ , but their contribution is estimated to be smaller than that of  $\sigma$ -donor bonding on the basis of theoretical considerations<sup>15,16)</sup> and systematic  $^{197}\text{Au}$ -Mössbauer studies of many gold(I) compounds.<sup>17-20)</sup> Thus, it is reasonable to conclude that the  $QS$  values mainly depend on the  $\sigma$ -donating ability of the ligands. On the other hand, it has been known that the  $IS$  value depends on the  $s$  electron density at the gold nucleus. The  $6s$  population directly increases the electron density at the nucleus, while the  $5d_{z^2}$  and  $6p_z$  populations decrease the electron density because of their shielding effect. The shielding effect of  $5d$  electrons is larger than that of  $6p$  electrons. The  $d_\pi$ -back-bonding reduces the  $d$  electrons and then increases the electron density at the  $^{197}\text{Au}$  nucleus. Increases in the  $s$  electron density at the nucleus lead to the increase in the  $IS$  value because of the positive  $\Delta R/R$  in  $^{197}\text{Au}$ -Mössbauer spectroscopy. Hence, both the  $QS$  and  $IS$  values depend on the  $\sigma$ -donating and  $\pi$ -accepting ability of the ligands. A linear relationship between the observed  $IS$  and  $QS$  values has been established for many gold(I) compounds.<sup>18,20,21)</sup>

The values of  $IS$  and  $QS$  for the gold(I) compounds with a  $\text{CN}$  group are expected to be larger than those for other gold(I) compounds. This expectation is confirmed by the observed large  $IS$  and  $QS$  values for  $\{[\text{R}_3\text{Sn}](\mu\text{-NC})[\text{Au}(\mu\text{-CN})]\}_x$  complexes. It can be concluded that the gold atom in these complexes is coordinated linearly with two cyano groups and forms an infinite one-dimensional polymeric structure.

## References

- 1) R. Uson, J. Fornies, M. A. Uson, and E. Lalinde, *J. Organomet. Chem.*, **185**, 359 (1980).
- 2) "Mössbauer Isomer Shift," ed by G. K. Shenoy and F. D. Wagner, North-Holland, Amsterdam (1978).
- 3) P. Gülich, R. Link, and A. Trautwein, "Mössbauer Spectroscopy and Transition Metal Chemistry," Springer-Verlag, Berlin (1978).
- 4) "Chemical Mössbauer Spectroscopy," ed by R. H. Herber, Plenum, New York (1985).
- 5) M. Katada, Y. Uchida, K. Sato, H. Sano, H. Sakai, and Y. Maeda, *Bull. Chem. Soc. Jpn.*, **55**, 444 (1982).
- 6) G. M. Bancroft and R. H. Platt., *Adv. Inorg. Chem. Radiochem.*, **15**, 59 (1972).
- 7) H. A. Stöckler and H. Sano, *Phys. Lett.*, **25A**, 550

- (1967); *Phys. Rev.*, **165**, 406 (1968); *Chem. Phys. Lett.*, **2**, 448 (1968); *J. Chem. Phys.*, **50**, 3813 (1969); *Polymer Lett.*, **7**, 67 (1969).
- 8) V. I. Gol'danskii and E. F. Makarov, "Chemical Applications of Mössbauer Spectroscopy," ed by V. I. Gol'danskii and R. H. Herber, Academic Press, New York (1968).
- 9) R. H. Herber, S. C. Chandra, and Y. Hazony, *J. Chem. Phys.*, **53**, 3330 (1970).
- 10) R. H. Herber and S. C. Chandra, *J. Chem. Phys.*, **54**, 1847 (1971).
- 11) R. H. Herber, *J. Chem. Phys.*, **54**, 3755 (1971).
- 12) S. Matsubara, M. Katada, K. Sato, I. Motoyama, and H. Sano, *J. Phys. Colloq.*, **C2**, 363 (1979).
- 13) H. D. Bartunik, W. Potzel, R. L. Mössbauer, and G. Kaendl, *Z. Phys.*, **240**, 1 (1970).
- 14) H. Prosser, F. E. Wagner, G. Wortmann, G. M. Kalvius, and R. Wäppling, *Hyperfine Intr.*, **1**, 25 (1975).
- 15) D. M. S. Esquivel, D. Guenzburger, and J. Danon, *Phys. Rev., B*, **19**, 1357 (1979).
- 16) T. K. Sham, R. E. Watson, and M. L. Perlman, *Phys. Rev. B*, **21**, 1457 (1980).
- 17) C. A. McAuliffe, R. V. Parish, and P. D. Randall, *J. Chem. Soc., Dalton Trans.*, **1977**, 1426.
- 18) P. G. Jones, A. G. Maddock, M. J. Mays, M. N. Muir, and A. F. Williams, *J. Chem. Soc., Dalton Trans.*, **1977**, 1434.
- 19) G. C. H. Jones, P. G. Jones, A. G. Maddock, M. J. Mays, P. A. Vergnans, and A. F. Williams, *J. Chem. Soc., Dalton Trans.*, **1977**, 1440.
- 20) R. V. Parish, *Gold Bull.*, **15**, 51 (1982).
- 21) Y. Uchida, M. Katada, H. Sano, H. Sakai, and Y. Maeda, *J. Radioanal. Nucl. Chem. Lett.*, **94**, 215 (1985).
-